High-spin states in ^{146}Sm

C. H. King,* B. A. Brown, and T. L. Khoo†
Cyclotron Laboratory and Department of Physics, Michigan State University, East Lansing, Michigan 48824
(Received 18 November 1977)

Transitions between states up to spin $16\hbar$ populated in the ^{146}Nd$(\alpha,4n)$ reaction were observed using γ-γ coincidence, γ-ray angular distribution and excitation function, and delayed γ-ray measurements. A level scheme was constructed up to 6.2 MeV with all levels above 3.8 MeV observed for the first time. Levels below 4.1 MeV were interpreted in terms of the coupling between two extra-core neutrons and excitations of the $N = 82$ core. Rotational structures and isomers were searched for above 4.1 MeV, but none were found.

[NUCLEAR REACTIONS: ^{146}Nd$(\alpha,4n\gamma)^{146}$Sm, E=47.9 MeV; measured E_γ, $I_\gamma(\theta)$, γ-γ coinc., α-γ delay, E_γ vs. E_α. ^{146}Sm deduced levels, J, π. Ge(Li) detectors. Enriched target.]

I. INTRODUCTION

Efforts to achieve a consistent understanding of the properties of heavy nuclei a few nucleons removed from a closed shell have been largely unsuccessful. Various collective models have achieved some success in special cases, but no single model has yet been devised which can describe all such nuclei. It appears that the properties of these nuclei depend sensitively on the underlying single-particle structure, and it may be that an adequate description may require a more microscopic approach such as a large-basis shell model calculation. However, as yet calculations utilizing a sufficiently large basis have been largely confined to light nuclei.

The isotopes of samarium are among the most extensively investigated of these transitional nuclei, perhaps because the stable isotopes represent a wide range of nuclear properties from the spherical nuclide ^{144}Sm, which has a closed neutron shell, to ^{154}Sm, which appears to be a relatively conventional deformed nuclide. Of all the samarium isotopes, ^{146}Sm, ^{147}Sm, and ^{148}Sm (N=84-86) have been among the most resistant to understanding in any simple collective model. The known low-lying properties of these nuclides have revealed no rotational bands and for the most part vibrational band sequences appear to be absent as well. Nevertheless, calculations of Bengtsson et al.[1] have indicated that the yrast states of ^{146}Sm should become significantly deformed at relatively low spins, and moreover that the deformation should be oblate, thus favoring the existence of the oblate yrast traps which have been predicted by Bohr and Mottelson.[2] In addition, the existence of shape coexistence[3] in the heavier samarium isotopes ^{150}Sm-^{152}Sm (N=88-90) suggests the possibility of deformed structures appearing in the lighter isotopes at sufficiently high excitation energy.

We have therefore undertaken an investigation of high-spin states in the nuclides ^{146,148}Sm using the $(\alpha,xn\gamma)$ reactions. The present paper reports the results of the ^{146}Sm investigation. Discussion of the ^{148}Sm results will appear in a subsequent report.[4]

II. EXPERIMENTAL PROCEDURE AND DATA ANALYSIS

The present study involved four separate measurements: 1) γ-ray angular distributions, 2) γ-γ coincidence, 3) γ-ray timing, and 4) γ-ray excitation functions. For all measurements, the target was a foil of neodymium metal with approximately 6 mg/cm^2 areal density and enriched to 97.5% in ^{146}Nd. The angular-distribution, coincidence, and timing measurements were all performed using a 47.9-MeV alpha beam from the Michigan State University cyclotron.

The γ-ray angular distributions were measured using a coaxial Ge(Li) detector with approximately 40 cm^3 active volume, placed about 12 cm from target. Singles γ-ray spectra were obtained at seven angles between 90° and 157° with respect to the beam direction. A sample spectrum is shown in Fig. 1. Normalization was obtained by using another Ge(Li) detector fixed at -90° as a monitor, with deadtime corrections accomplished by feeding a beam-current digitizer output into the ADC's used for the pulse-height spectra of each detector. An effort was made to extract accurate γ-ray energies by performing separate runs with ^{75}Se, ^{166m}Ho, ^{137}Cs, and ^{60}Co sources near the detector during the collection of a ^{146}Nd + α spectrum and using the known[5] energies of the lines in these sources to determine the energies of the ^{146}Nd + α lines. The measured γ-ray energies listed in Table I are believed to be accurate to better than 0.1 keV for isolated peaks. The γ-ray excitation functions were obtained by taking singles spectra with the 40-cm^3 detector at a fixed angle of 125° for three other energies: 40, 45.8, and 49.8 MeV. For all spectra, photopeak areas were determined by using the peak-fitting program SAMPO.[6]

The angular distributions were fitted using the usual Legendre polynomial expansion:

$$W(\theta)=I_\gamma(1+A_2P_2(\cos\theta)+A_4P_4(\cos\theta)).$$

The γ-ray intensities I_γ and the A_2 and A_4 coefficients are listed in Table I. It was found that for this, and a ^{148}Nd$(\alpha,4n\gamma)^{148}$Sm experiment performed at the same time, the extracted A_2 coefficients for known stretched-E1 and stretched-E2 transitions depopulating the same level were attenuated by significantly different amounts from the expected values for maximum alignment.[7] However, a correction term of +0.05 added to the A_2 coefficients was found to yield consistent A_2 attenuation coefficients within uncertainties for all strong, well-resolved transitions. The A_2 coefficients listed in Table I have been corrected by this amount and an estimate of the uncertainty in this procedure is included in the quoted uncertainties. The attenuation factors for the extracted

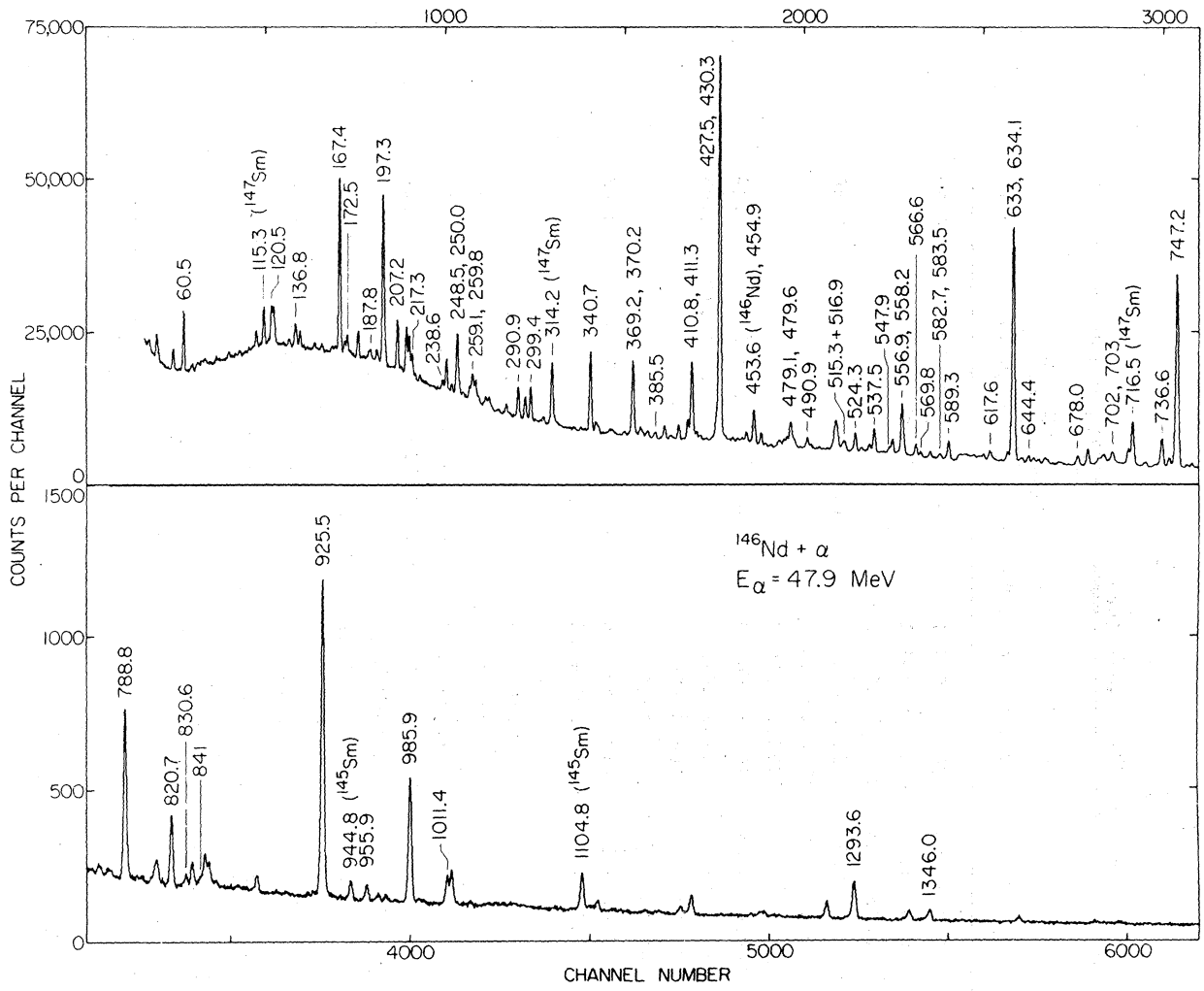

FIG. 1. In-beam γ-ray spectrum in a Ge(Li) detector at 125° with respect to the beam from the bombardment of a ^{146}Nd target by 47.9 MeV α particles.

A_4 coefficients of strong stretched-E2 transitions were consistent (given the usual gaussian assumption for the angular momentum substate populations[7]) with those for the corrected A_2 coefficients of the same transitions within uncertainties. Thus, no corrections to the A_4 coefficients seem to be required.

The coincidence measurements were carried out using two coaxial Ge(Li) detectors (40 cm^3 and 60 cm^3 active volume) placed at +90° and -90° with respect to the beam direction and approximately 2.5 cm from the target. The pulse heights from each detector and time-to-amplitude converted (TAC) signals indicating the time separation between the two γ-rays were recorded on magnetic tapes in a three-parameter event-by-event mode. The data consisted of about 2.7 x 10^7 events, and the tapes were scanned with windows set on the photopeaks of γ rays in the pulse-height spectrum from one detector and on the prompt portion (approximately 50 ns wide) of the TAC spectrum. Subtraction for random coincidences was performed by setting windows away from the prompt peak in the TAC spectrum, and that for Compton background, by setting windows on regions above and below the photopeaks in the pulse-height spectrum. The spectra obtained from five sample gates are shown in Fig. 2.

The γ-ray timing measurement was performed by using the 60-cm^3 Ge(Li) detector in the same geometry as in the coincidence measurement. The TAC was started by the Ge(Li) signals and stopped by a signal from the cyclotron rf. Delayed γ-ray spectra were then generated on line by dividing the portion of the TAC spectrum between cyclotron beam bursts (48ns) into nine bins and using these to gate the Ge(Li) signals. Delayed γ-rays from ^{146}Sm were observed in only one spectrum, and the energies and relative intensities correspond to decay from the 2797.6 (9^-) level. We have estimated that the half life of this state is between 0.6 and 1.6 nsec and that other levels populated with significant strength in the ^{146}Nd(α,4n) reaction have half lives shorter than ~ 0.6 nsec.

The ^{146}Sm level scheme derived from these measurements is shown in Fig. 3. The placement of all γ-ray transitions indicated with solid lines was based on the coincidence data, with the singles and coincidence intensities used to determine the ordering. The dotted lines correspond to transitions for which the evidence in the coincidence data is very weak or which appear in the

TABLE I. Summary of ^{146}Nd(α,4nγ) Data

E_γ[a] (keV)	I_γ[b] (rel. int.)	A_2[c]	A_4[c]	Assignment	$I_\gamma^{E}/I_\gamma^{49.8\ MeV}$ (rel. int.)[g] E(MeV) = 40	45.8	47.9
60.5	18.6	-0.23±0.02	-0.02±0.03	2797.6→2737.1	0.51	0.86	0.90
120.5±0.2	2.4	-0.17±0.02	0.01±0.03	4461.4→4341.1			
136.8	1.3	-0.22±0.10	0.05±0.15	2737.1→2600.3			
167.4	11.8	-0.17±0.01	0.01±0.02	4628.8→4461.4	0.20	0.72	0.86
172.5	1.4	-0.15±0.05	0.02±0.08	4752.2→4579.7			
187.8±0.2[f]	(1.0±0.5)			3354.5→3166.8			
197.3[f]	13.4	0.26±0.03	-0.05±0.04	2797.6→2600.3	0.76[f]	0.87[f]	0.94[f]
207.2	4.1	-0.19±0.03	-0.01±0.05	4202→3995		0.89±0.10	0.98
217.3	2.1	-0.26±0.04	-0.03±0.06	4969.5→4752.2			
238.6	1.0	-0.13±0.07	-0.06±0.10	4579.7→4341.1			
248.5	6.2	-0.10±0.03	0.02±0.05	5218.0→4969.5	0.15±0.02	0.67	0.82
250.0±0.2	1.2	0.42±0.13	-0.04±0.19	4341.1→4091.2			
259.1±0.3[d,f]	(1.2±0.7)			4461.4→4202			
259.8±0.3[d,f]	(1.4±0.7)			5874→5614.0			
271.6±0.5[f]	0.5±0.5			2083→1811.5			
290.9	3.9	-0.15±0.03	-0.01±0.05	4752.2→4461.4	0.17±0.02	0.76	0.90
299.4	4.3	-0.02±0.02	0.02±0.03	5517.5→5218.0	0.17±0.02	0.65	0.82
305.5±0.5	0.3±0.3			3043→2737.1			
340.7	12.4	-0.07±0.02	-0.01±0.03	4969.5→4628.8	0.22	0.69	0.86
369.2±0.2	(1.5±1.0)	-0.01±0.03	0.00±0.04	3166.8→2797.6	0.26	0.76	0.89
370.2	(13.0±1.0)			4461.4→4091.2			
385.5[f]	≤1.0	-0.07±0.09	-0.11±0.13	3183.1→2797.6	2.15±0.38[f]	1.38±0.25[f]	1.29±0.23[f]
410.8±0.3[d]	(11±2)	0.11±0.01	0.01±0.02	2222→1811.5			
411.3±0.3[d]	(9±2)			4195→3783.5			

TABLE 1. (*Continued*)

E_γ[a] (keV)	I_γ[b] (rel. int.)	A_2[c]	A_4[c]	Assignment	$I_\gamma^{E}/I_\gamma^{49.8\ MeV}$ (rel. int.)[g] E(MeV) = 40	45.8	47.9
427.5±.2	3.6±0.8	-0.12±0.04	0.07±0.05	3995→3567			
430.3	83.0	0.32±0.02	-0.08±0.03	1811.5→1381.2	0.78	0.95	0.97
442.4±0.3	0.6±0.4			3043→2600.3			
454.9±0.3[d,f]	(1.8±1.0)			5972→5517.5			
479.1±0.3[d,f]	(3.7±1.0			5697→5218.0			
479.6±0.3[d,f]	(1.5±0.5)			6177→5697		0.43	0.66
490.9	2.8	0.36±0.05	-0.09±0.08	5697→5206	0.47±0.08	0.65	0.77
515.3±0.8[d]	(0.8±0.8)			2737.1→2222			
516.9±0.2	2.6	0.32±0.04	-0.02±0.06	2600.3→2083			
524.3	5.3	-0.02±0.02	0.00±0.03	3567→3043	0.77±0.10	0.92	0.99
537.5	6.9	0.33±0.03	-0.08±0.05	4628.8→4091.2		0.73	0.86
547.9±0.2	1.5	0.47±0.13	-0.35±0.21	5517.5→4969.5			
556.9	(18.0±1.0)			3354.5→2797.6			
558.2±0.3	(1.5±1.0)	0.39±0.01	-0.02±0.02	4341.1→3783.5		0.84	0.92
566.6[g]	4.0	-0.31±0.05	-0.01±0.07	3166.8→2600.3	0.71±0.09[f]	0.91[f]	0.96[f]
569.9[g]	1.5	0.33±0.03	-0.07±0.05	3924.4→3354.5	1.04±0.19[f]	0.93[f]	0.96[f]
582.7±0.3[d,f]	(0.9±1.0)			3183.1→2600.3			
583.5±0.3[d,f]	(0.8±1.0)	-0.53±0.08	0.01±0.11	2667→2083	1.35[f]	1.08[f]	0.98[f]
589.3±0.2[f]	(2.7±0.5)			5218.0→4628.8	0.61[f]	0.69[f]	0.82[f]
617.6±0.5[f]	(1.8±0.5)			3354.5→2737.1			
633.0	($9.5 \geq I_\gamma \geq 2.5$)			1380→747.2			
634.1	($91.5 \geq I_\gamma \geq 84.5$)	0.31±0.01	-0.08±0.02	1381→747.2	0.92	0.99	1.00
644.4	2.5	-0.32±0.09	0.00±0.14	5614.0→4969.5		0.53	0.84
678.0±0.3[d,f]	(2.0±0.7)			4461.4→3783.5	5.35[f]	1.27[f]	1.04[f]

TABLE 1. (*Continued*)

E_γ[a] (keV)	I_γ[b] (rel. int.)	A_2[c]	A_4[c]	Assignment	$I_\gamma^E/I_\gamma^{49.8\ MeV}$ (rel. int.)[g] E(MeV) = 40	45.8	47.9
702.2[d]	(4.3±0.8)	0.00±0.05	-0.01±0.08	2083→1381.2			
703.1[d]	(3.2±0.8)			2083→1380			
736.7	14.6	0.29±0.03	-0.09±0.05	4091.2→3354.5		0.78	0.87
747.2	100.	0.31±0.01	-0.07±0.02	747.2→0.0	1.00	1.00	1.00
754.2±0.2	1.2	0.48±0.25	0.28±0.37	3354.5→2600.3		0.76±0.12	1.11±0.15
757.6	1.8	0.56±0.13	0.00±0.20	3924.4→3166.8		0.95	0.99
788.8	21.2	-0.21±0.01	0.02±0.02	2600.3→1811.5	0.70	0.94	0.99
820.7[f]	9.0	0.33±0.02	-0.10±0.03	3043→2222	1.46[f]	1.08[f]	1.03[f]
830.6±0.3[f]	≤1.2			3567→2737.1	11.47±3.1[f]	1.84±0.53[f]	1.21±0.34[f]
841.0±0.5[f]	1.4±0.7			2222→1381.2			
925.5	50.9	0.33±0.01	-0.10±0.02	2737.1→1811.5	0.67	0.90	0.97
955.9	2.7	-0.13±0.07	0.01±0.10	3753.5→2797.6	0.56±0.08	0.91	1.02
985.9	22.1	0.36±0.02	-0.10±0.04	3783.5→2797.6	0.41	0.84	0.94
1011.4	4.5	0.30±0.05	-0.08±0.08	5206→4195		0.69	0.85
1231.2±0.3	0.9	0.39±0.18	-0.18±0.23	3043→1811.5			
1293.6	10.3	0.32±0.04	-0.13±0.08	4091.2→2797.6	0.35±0.06	0.78	0.90
1346.0	3.0	0.29±0.09	-0.13±0.13	5129.9→3783.5		0.86	0.96

[a] Uncertainty ±0.1 keV unless specified.
[b] Taken at 47.9 MeV. Uncertainty ±10% unless specified. Numbers in parentheses represent estimates based on coincidence intensities.
[c] See the discussion in Sec. II of the text concerning the A_2 and A_4 coefficients.
[d] Energy taken from coincidence spectra.
[e] Not isolated in present experiment. Energy taken from ref. 9.
[f] Unresolved from other lines not in ^{146}Sm.
[g] Uncertainty ±10% unless specified.

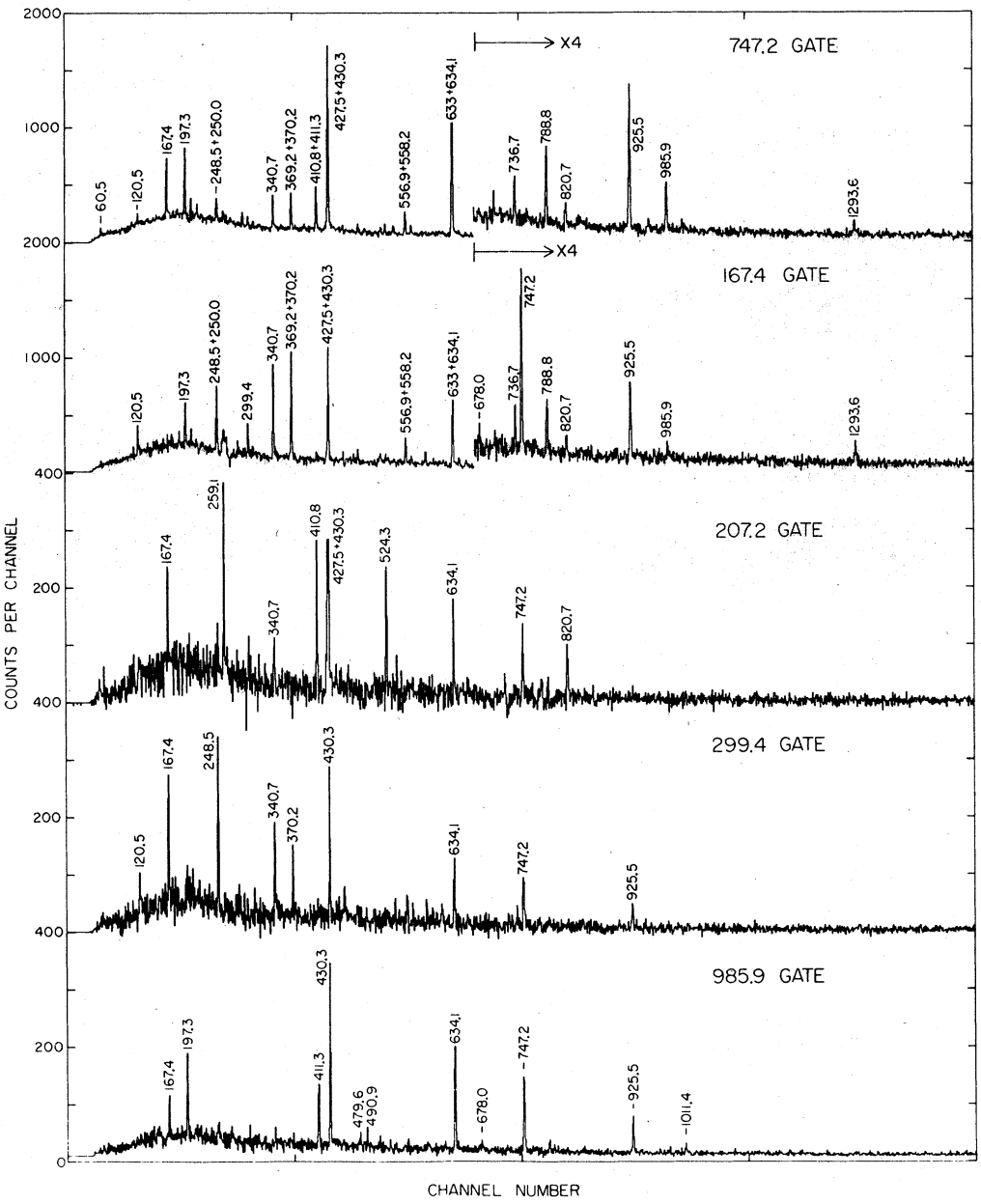

FIG. 2. Sample γ-γ coincidence spectra.

singles spectra but which are too weak to appear in the spectra of the coincidence gates. All possible dipole and quadrupole transitions between levels below 3600 keV excitation have been searched for in the singles spectra. Transitions between states above this energy are all based on the coincidence data. Several peaks in the spectra correspond to multiplets of γ-ray lines which could not be resolved using the peak-fitting program. For these lines, the approximate energies and relative intensities were determined from the coincidence data.

The spin assignments of the levels are based primarily on the measured A_2 and A_4 coefficients combined with the assumption that levels near the yrast line tend to be preferentially populated in fusion-evaporation reactions. Hence, most γ-ray transitions will be from a higher to a lower spin state. The excitation-function data were used as an additional check on the spin sequence in a γ-ray cascade, since higher-spin levels will tend to be more easily populated at higher energies than the lower-spin levels due to the higher angular momentum of the compound nucleus. The excitation functions of the relative γ-ray intensities for the strongest lines, normalized to 1.0 at 49.8 MeV, are shown in Table I. Since the angular-distribution coefficients can at best determine only the multipolarity and not the parity of the γ rays, parity assignments were made only by using transitions

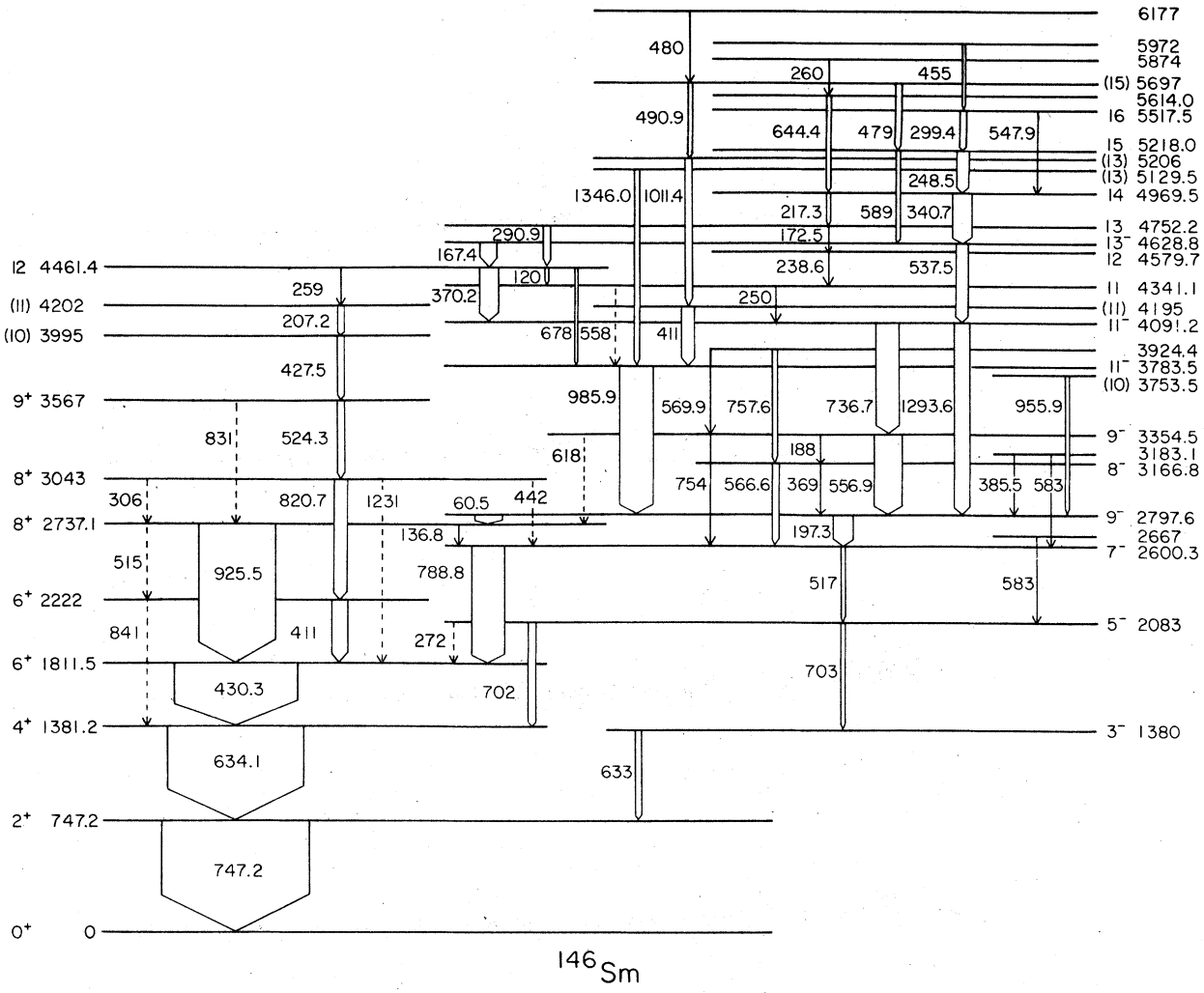

FIG. 3. ^{146}Sm level scheme. The solid lines indicate transitions determined entirely from the γ-γ coincidence data. The dotted lines correspond to transitions for which the coincidence data gave only weak evidence or which appeared only in the singles spectra.

with A_2 and A_4 coefficients consistent with stretched-quadrupole transitions, which were assumed to be E2.

III. DISCUSSION

A. Comparison with other ^{146}Sm data

Low-spin ($I \leq 6\hbar$) levels in ^{146}Sm are populated in the decays of ^{146}Eu and ^{146}Pm. Measurements[8,9] of γ rays and conversion electrons following these decays have resolved the 634 and 633 keV as well as the 702 and 703 keV lines and thus have established the existence of the $1381(4^+)$-$1380(3^-)$ doublet. Since these lines were unresolved in the present data, we have used the earlier measurements to infer the existence of this doublet. The spin assignments and γ-ray transitions involving the few other low-spin levels seen in this experiment are in accord with the assignments from the decay studies, and the spin assignments are in accord with other experiments populating low-spin levels such as two-nucleon[10] and single-nucleon[9,11] transfer reaction studies.

Transitions involving levels up to $I=11\hbar$ and 3.8 MeV excitation energy have been observed in ^{144}Nd(α,2n) experiments by Singh and Johns[9] and Kownacki et al.[12] Kownacki et al. have so far reported[12] only the yrast transitions, and our assignments agree with theirs up to the $2737(8^+)$ level. However, they place the 985.9 keV γ ray as feeding directly into this 8^+ level, thus inferring a 10^+ state at 3723 keV. Our coincidence data are clearly in disagreement with such an assignment, as can be observed in Fig. 2 where a strong 197.3 keV line appears in the spectrum of the 985.9 keV coincidence gate. This, as well as the appearance of a 985.9 keV coincidence in the 60.5 keV gate and the absence of coincidences between the 197.3 keV and 925.5 keV lines, supports our assignment of the 985.9 keV line as the $3783.5(11^-)$ to $2797.6(9^-)$ transition, with the 60.5 keV transition connecting the $2797.6(9^-)$ and $2737.1(8^+)$ states (see Fig. 3). Singh and Johns agree with this assignment. Thus, we suggest that the $3723(10^+)$ state of Kownacki et al. is spurious.

On the other hand, Singh and Johns suggest that the 986 keV line is a doublet with one component feeding

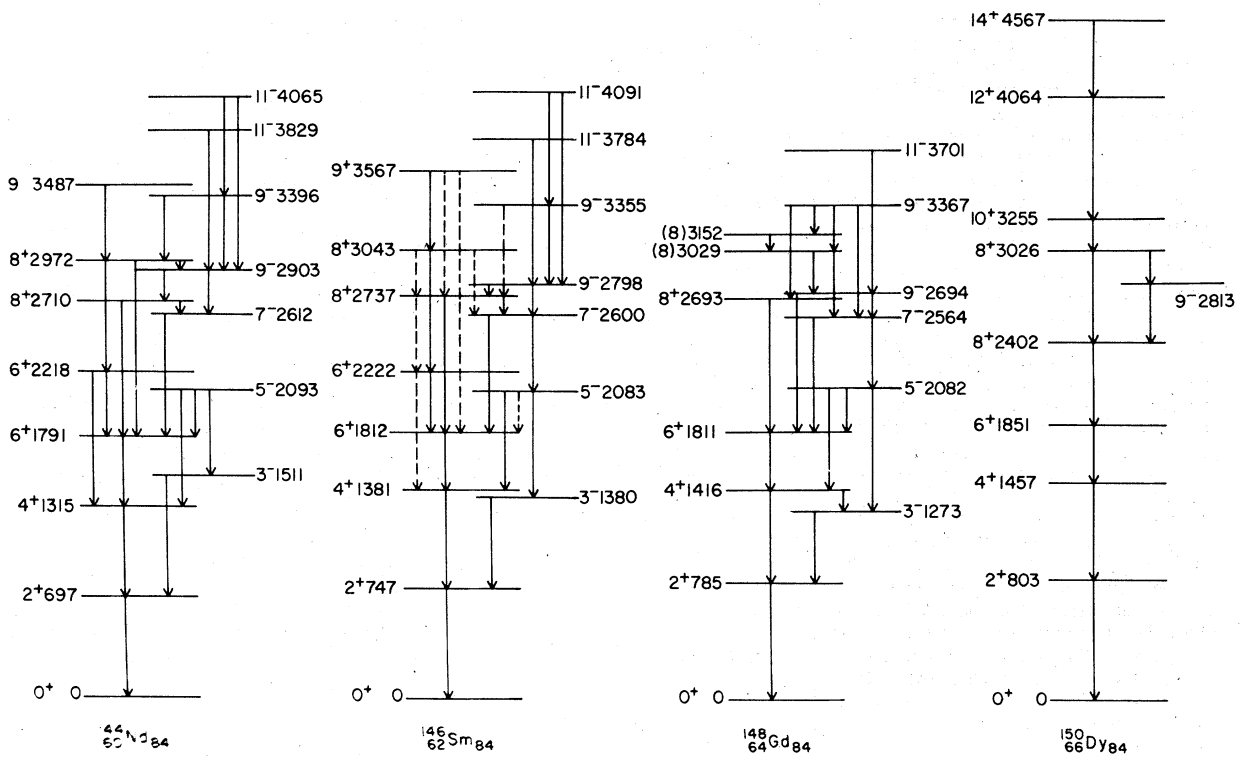

FIG. 4 Comparison of selected levels and transitions in the N=84 isotones ^{144}Nd, ^{146}Sm, ^{148}Gd, and ^{150}Dy. The ^{144}Nd data are taken from refs. 13 and 14, the ^{148}Gd data from refs. 15 and 16, and the ^{150}Dy data from ref. 17.

directly into the 2222(6^+) state, presumably based on the strong coincidence with the 411 keV line. Although we cannot rule out this possibility from our data, there is no evidence in our spectra that the 986 keV peak is a doublet. The 411 keV peak is, however, clearly a doublet. We therefore prefer to attribute the strong 986-411 coincidence to a component of the 411 keV peak feeding into the 3783.5(11^-) state, as is indicated in Fig. 3. This is supported by the fact that the energy of the 411 keV peak in the 985.9, 1011.4, and 490.9 keV gates is consistently higher than that in the 207.2, 524.3, and 820.7 keV gates, which suggests that the 411 keV γ rays in coincidence with these two cascades come from different transitions.

The only other major discrepancies between our assignments and those of Singh and Johns concern the 3043 keV state and the transitions feeding it. The angular distribution coefficients we measured for the 820.7 keV transition (see Table I) are consistent with those for a stretched E2 and hence we have given an 8^+ assignment to the 3043 keV state. In their ^{144}Nd(α,2n) experiment, Singh and Johns measure an A_2 coefficient for this transition significantly larger than that expected for a stretched E2, and using this information together with arguments of systematics with other Sm isotopes give a 6^+ assignment to the 3043 keV level. It should be noted that the excitation function we measure for the 820.7 keV intensity indicates a possible weak additional component to this line from γ rays not in ^{146}Sm, and this may account for the discrepancy between our two measurements. On the other hand, the 3043 keV state is fed from the 4461.4 keV state through the 259-207.2-427.5-524.3 cascade, and the spin of the latter state is established to be $12\hbar$ based on the strong transitions between the negative-parity states shown on the right-hand side of Fig. 3. Moreover the angular distributions of the 259, 207.2, 427.5 and 524.3 keV transitions appear to require spin change $\Delta I < 2\hbar$. Thus, it is unlikely that the spin of the 3043 keV state is less than $8\hbar$. In addition, systematics with other N=84 isotones, as shown in Fig. 4, make an 8^+ assignment plausible as well.

As for the cascade feeding the 3043(8^+) state, Singh and Johns observe the 207.2 and 524.3 keV transitions but not the 259 and 427.5 keV transitions. The 259-keV transition was missed, presumably because the spin of the 4461.4 keV state is too high for this state to be populated in an (α,2n) reaction. The 427.5 keV line is barely resolvable in our spectra from the strong 430.3 keV line, and since it should be weaker in the (α,2n) reaction, it is not too surprising it was not found. Coincidence gates we have set on 820.7, 524.3, 427.5, 207.2, and 259 keV lines clearly indicate that the 427.5 keV transition is a member of the cascade. The 524.3 keV transition can be placed at the bottom of the cascade and the 259 keV transition at the top based on singles intensities. The ordering of the 427.5 and 207.2 keV γ rays is ambiguous. We have placed the 207.2 transition above the 427.5 based on the equality of the 427.5 and 430.3 intensities in the 207.2 gate. However, our data are not inconsistent with the other ordering.

B. States below 4.1 MeV

A comparison between some of the yrast and near yrast levels of the N=84 nuclides is shown in Fig. 4. These

include the levels determined in the present and other studies of ^{146}Sm together with levels from in-beam γ-ray studies[13-17] of ^{144}Nd, ^{148}Gd, and ^{150}Dy. ^{140}Ba and ^{142}Ce levels are only known[18,19] for $I \leq 4\hbar$ and thus were not included in the figure.

The similarities in structure among these nuclides are quite striking. One common feature is the 0_1^+-2_1^+-4_1^+-6_1^+ structure, with the energy spacing decreasing with spin. Since the first neutron orbit outside the N=82 closed shell is $2f_{7/2}$, it is natural to interpret this in terms of a $(2f_{7/2})^2$ configuration. However, the E(I)/E(I_{max}) ratios are much smaller than one expects for a pure two-particle configuration, suggesting that significant particle-core interactions and/or admixtures of other valence orbits are important. Calculations of the structure of the N=84 nuclides in which interactions are explicitly included between the extra-core nucleons and vibrational excitations of the core have been carried out by Heyde and Brussard[20] and by Vanden Berghe.[21] (The latter calculation included the p,f, $h_{9/2}$ and $i_{13/2}$ orbitals). For the positive-parity states in both calculations, only quadrupole vibrations of the core were allowed with one-, two-, and three-phonon states included. These calculations indicate large mixing among the valence $(2f_{7/2})^2$, $(2f_{7/2},3p_{3/2})$ and $(3p_{3/2})^2$ and core-excited configurations.

The excitation energies and wave functions calculated by Vanden Berghe for the 0^+, 2^+ and 4^+ states are given in Ref. 21. His results[22] for the 6^+ and 8^+ states are given in Table II. The excitation energies of the 6_1^+, 8_1^+ and 8_2^+ states are in good agreement with experiment. Our 6_2^+ state at 2222 keV may correspond to the coupling of the two valence neutrons to the 2323-keV 6^+ state in ^{144}Sm; this configuration was not included in Vanden Berghe's basis set. However, the strong $8_2^+ \rightarrow 6_2^+$ transition relative to the $8_2^+ \rightarrow 6_1^+$ transition cannot be understood unless either both the 8_2^+ and 6_2^+ states correspond to those calculated by Vanden Berghe or both correspond to I =6 or 8$\hbar$ excitations of the protons in ^{144}Sm as suggested by the comparison in Fig. 5. It will be interesting in the future to extend this calculation to include more than the 2^+ phonon in ^{144}Sm and to calculate electromagnetic transition matrix elements between these high spin states.

Higher spin positive parity states up to I=12$\hbar$ can be explained in terms of the $(i_{13/2})^2$ configuration, but again mixing with core-excited configurations are probably important. The effect of the core excitations probably accounts for the difference between ^{150}Dy and the other N=84 nuclides in the structure above the second 8^+ state. The closure of the $2d_{5/2}$ proton shell[17] at Gd(Z=64) makes $1h_{11/2}$ the valence proton orbit in Dy (Z=66) and allows for a low-lying 10^+ state with a $(1h_{11/2})^2$ configuration in ^{150}Dy.

The negative parity states in the N=84 isotones are also quite similar. These states can be qualitatively interpreted in terms of coupling between the positive parity levels and the 3^- octupole vibration. This is illustrated in Fig. 5 where the negative parity levels up to I =11 are placed next to the positive parity levels, with the energy of the 3^- excitation removed. The depression of the negative parity stretched states relative to the positive parity states can be interpreted as resulting from the interaction between the positive-parity and octupole excitations. Explicit calculations for the case of the $2^+ \otimes 3^-$ multiplet have been carried out[21,23] and have obtained a reasonably good reproduction of the experimental spectrum.

In this context, it is interesting to compare the E1/E2 branching ratios from the negative-parity levels in ^{146}Sm and ^{144}Nd with those expected in the interacting boson model.[24] In this model,

$$\frac{B[E1;(I=2n+3)^- \rightarrow (I=2n+2)^+]}{B[E2;(I=2n+3)^- \rightarrow (I=2n+1)^-]} = \frac{n+1}{n} c$$

where c is a constant which depends on the nucleus. In Table III, we compare the predictions of this model with our measured values, where we have fixed c to give the correct

$$B[E1;5^- \rightarrow 4^+]/B[E2;5^- \rightarrow 3^-]$$

branching ratio. As can be seen, while the ^{146}Sm and ^{144}Nd branching ratios agree, the interacting boson model is in disagreement, especially for the 9^- branching ratio. This is not particularly surprising in nuclei only two neutrons away from a closed shell.

TABLE II. Wave functions obtained by Vanden Berghe (Ref. 22) for higher spin states which were not listed in Ref. 21. The notation is the same as in Ref. 21.

1812 keV $|6_1^+\rangle = 0.68\,|(f_{7/2})^2 6;00\rangle - 0.29\,|(p_{3/2},f_{7/2})4;12\rangle - 0.33\,|(f_{7/2})^2 4;12\rangle - 0.37\,|(f_{7/2})^2 6;12\rangle$

2769 keV $|6_2^+\rangle = -0.28\,|(f_{7/2})^2 6;00\rangle + 0.25\,|(f_{7/2}h_{9/2})6;00\rangle - 0.50\,|(f_{7/2})^2 4;12\rangle + 0.28\,|(f_{7/2})^2 6;12\rangle - 0.30\,|(f_{7/2})^2\ 0;36\rangle$

2781 keV $|8_1^+\rangle = 0.38\,|(f_{7/2}h_{9/2})8;00\rangle - 0.70\,|(f_{7/2})^2 6;12\rangle - 0.24\,|(f_{7/2}h_{9/2})8;12\rangle + 0.27\,|(p_{3/2}f_{7/2})4;24\rangle + 0.24\,|(f_{7/2})^2 4;24\rangle + 0.22\,|(f_{7/2})^2 6;24\rangle$

3049 keV $|8_2^+\rangle = 0.65\,|(f_{7/2}h_{9/2})8;00\rangle + 0.41\,|(f_{7/2})^2 6;12\rangle - 0.46\,|(f_{7/2}h_{9/2})8;12\rangle$.

C. States above 4.1 MeV

Above the second 11^- state in ^{146}Sm, a large number of high-spin states are populated in the $(\alpha,4n)$ reaction. Many more levels are observed up to a higher excitation energy than in any of the N=84 nuclides so far studied. Indeed, more levels appear than can easily be accounted for in terms of the simple coupling schemes described in the last section. For example, five spin 11 states appear between 3.7 and 4.3 MeV, only two of which can easily be explained by coupling the octupole vibration to known positive parity structures. It is likely that more complicated models will be required to explain the observed structure.

On the other hand, it is interesting that we have observed no rotational structures, although we see transitions between states up to 6.2 MeV. Not only do the energy levels fail to follow any rotational pattern but also the transitions indicate a lack of quadrupole collectivity in the dominance of $\Delta I = 1\hbar$ over $\Delta I = 2\hbar$ transitions.

The lack of rotational bands should not necessarily be construed as evidence that ^{146}Sm remains spherical up to the excitation energies observed. Should the nucleus become oblate, as has been predicted,[1,25] the yrast levels are expected to be a sequence of intrinsic, rather than rotational, states. The energies of intrinsic states should, on the average, be given by $E \sim \frac{\hbar^2}{2\mathcal{I}_{rigid}} I(I+1)$, where $\mathcal{I}_{rigid}$ corresponds to the moment of inertia for rigid body rotation about the symmetry axis.[2] On the other hand, the moment of inertia associated with collective rotation about an axis perpendicular to the

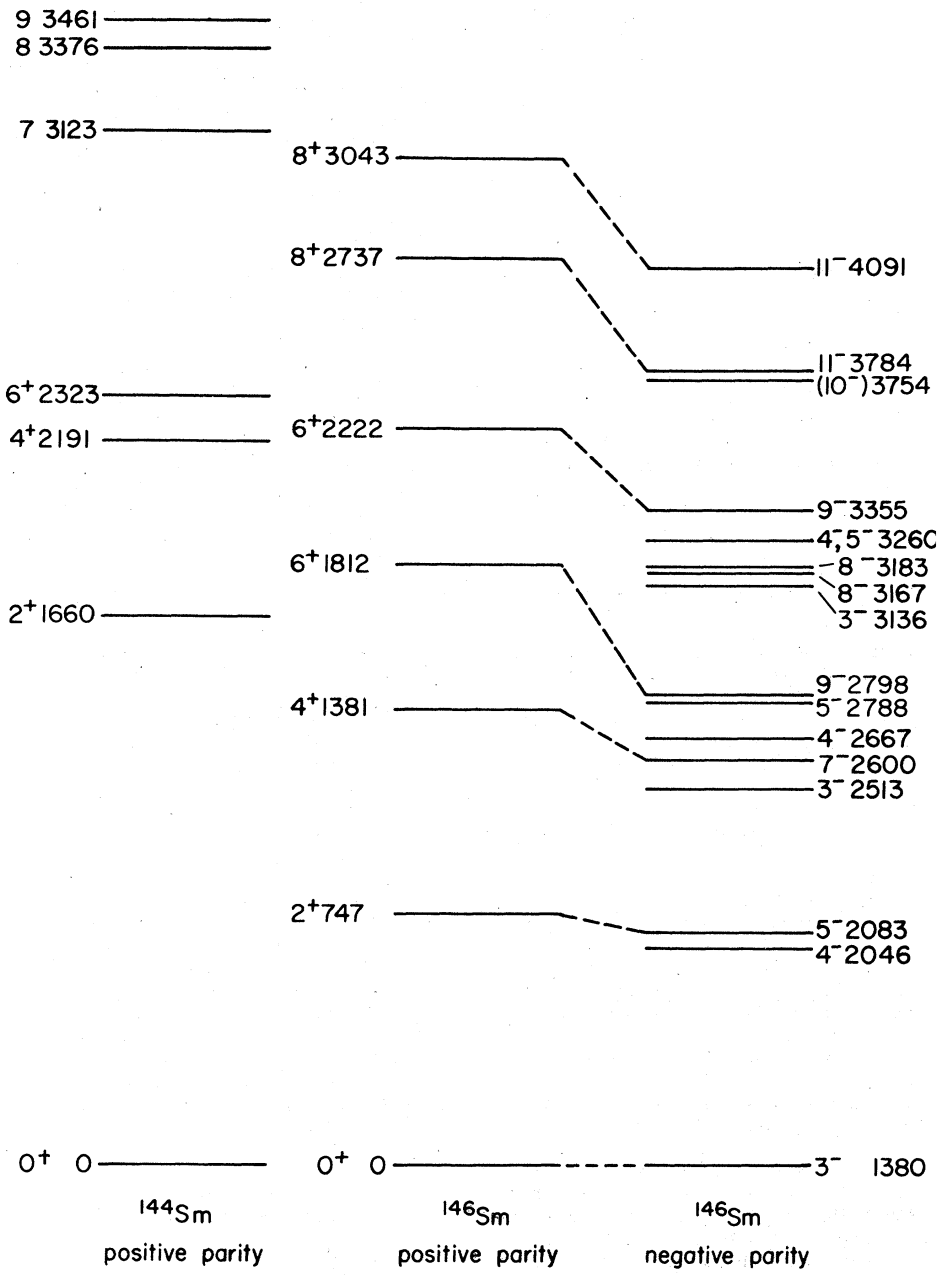

FIG. 5. Comparison of positive-parity levels in ^{144}Sm (data from ref. 26) with positive-parity levels in ^{146}Sm and negative-parity levels in ^{146}Sm with energies lowered to put the 3^- state at the same energy as the ground state. The dashed lines indicate the stretched negative parity states tentatively associated with the positive parity states.

symmetry axis is considerably smaller because of pairing effects. As a consequence, rotational bands in an oblate nucleus are not expected to be yrast and, hence, not favourably populated in the $(\alpha,4n)$ reaction employed in this study.

Therefore, it is difficult to distinguish between oblate and spherical shapes unless they are manifested through significantly different shell-effects in the two cases. One possible signature of oblateness is the occurrence of high spin states, such as yrast traps, at lower energies than might be expected with a spherical core. However, as was mentioned in Sec. II, no high spin isomers were observed (for $I \leq 16\hbar$) despite indications[1] that ^{146}Sm might be a likely candidate for yrast traps. This is perhaps not too surprising in view of more recent calculations[25] which indicate that such isomers should not occur until $I=53\hbar$.

TABLE III. Comparison of E1/E2 Branching Ratios.[a]

	^{146}Sm	^{144}Nd[b]	IBA[c]
$\frac{B(E1;5_1^- \to 4_1^+)}{B(E2;5_1^- \to 3_1^-)}$	1	1	1
$\frac{B(E1;7_1^- \to 6_1^+)}{B(E2;7_1^- \to 5_1^-)}$	0.9±0.1		0.75
$\frac{B(E1;9_1^- \to 8_1^+)}{B(E2;9_1^- \to 7_1^-)}$	2.8±0.4	3.1±1.1	0.67

[a] Normalized so that $B(E1;\ 5^- \to 4^+)/B(E2;5^- \to 3^-) \equiv 1$.

[b] Ref. 13.

[c] Ref. 24.

IV. CONCLUSION

We have studied the nuclide ^{146}Sm using the ^{146}Nd(α,4n)^{146}Sm reaction, measuring γ-γ coincidence, γ-ray angular distributions and excitation functions, and delayed γ-rays between beam bursts. A level scheme for this nuclide was constructed up to 6.2 MeV and spin 16ħ. Below 4.1 MeV, the levels, like those in other N=84 nuclides, can be understood in terms of coupling the two extra-core neutrons to excitations of the N=82 core. Above this energy many high spin levels appear which are difficult to account for in such a model and which also do not appear to be grouped in rotational bands. No isomers were observed above 4.1 MeV.

ACKNOWLEDGMENTS

This research was supported in part by the U.S. National Science Foundation. We are grateful to Y.K. Peng and D.G. Burke of McMaster University for providing us with metallic ^{146}Nd, and to G. Vanden Berghe for communicating to us the results of his calculations.

*Present address: Nuclear Science Division, Lawrence Berkeley Laboratory, University of California, Berkeley, CA 94720, USA.

†Present address: Physics Division, Argonne National Laboratory, Argonne, IL 60439, USA.

[1] R. Bengtsson, S.E. Larsson, G. Leander, P. Möller, S.G. Nilsson, S. Åberg, and Z. Szymański, Phys. Lett. 57B, 301(1975).

[2] A. Bohr and B.R. Mottelson, Physica Scripta 10A, 13(1974).

[3] S. Hinds, J. Bjerregaard, O. Hansen, and O. Nathan, Phys. Lett. 14, 48(1965); W. McLatchie, N. Darcey, and J.E. Kitching, Nucl. Phys. A159, 615(1970).

[4] B.A. Brown, T.L. Khoo, and C.H. King, (unpublished).

[5] R.L. Heath, Gamma-Ray Spectrum Catalogue, Idaho National Engineering Laboratory, Aerojet Nuclear Company, Idaho Falls, Idaho.

[6] J.T. Routti and S.G. Pussin, Nucl. Inst. Meth. 72, 125(1969).

[7] E. der Mateosian and A.W. Sunyar, Atomic Data and Nucl. Data Tables 13,391 and 407(1974).

[8] D.J. Buss, E.G. Funk, and J.W. Mihelich, Phys. Rev. 141, 1193(1966); M.P. Avotina, E.P. Grigor'ev, A.V. Zolotavin, and V.O. Sergeev, Phys. Lett. 19, 310(1965) and Sov. J. Nucl. Phys. 5, 325(1967); C.J. Paperiello, D.J. Buss, E.G. Funk, and J.W. Mihelich, Nucl. Phys. A121, 191(1968); and S. Antman, H. Pettersson, Z. Zehlev, and I. Adam, Z. Physik 237, 285(1970).

[9] B. Singh and M.W. Johns, Can. J. Phys. 53, 391 (1975).

[10] J.H. Bjerregaard, O. Hansen, O. Nathan, and S. Hinds, Nucl. Phys. 86, 145(1966); P. Debenham and N.M. Hintz, Nucl. Phys. A195, 385(1972); and W. Oelert, G. Lindström, and V. Riech, Nucl. Phys. A233, 237(1974).

[11] W. Oelert, J.V. Maher, D.A. Sink and M.J. Spisak, Phys. Rev. C12, 417(1975).

[12] J. Kownacki, Z. Sujkowski, H. Ryde, and I. Adam, Proceedings of the Int. Conf. on Nuclear Structure and Spectroscopy, Amsterdam, 1974, eds. H.P. Blok and A.E.L. Dieperink (Scholar's Press, Amsterdam, 1974) p. 103.

[13] L.-E. De Geer, A. Kerek, Z. Haratym, J. Kownacki, and J. Ludziejewski, Nucl. Phys. A259, 399(1976).

[14] J.J. Berzins, et al., Gemeinsamer Jahresbericht 1976, Zentral institut für Kernforschung, Rossendorf bei Dresden, DDR, p. 39.

[15] K. Krien, F. Djadali, R.A. Naumann, H. Hübel, and E.H. Spejewski, Phys. Rev. C 7, 2484(1973).

[16] S. Lunardi, M. Ogawa, M.R. Maier, and P. Kleinheinz, Annual Report 1976, Institut für Kernphysik, Kernforschungsanlage Jülich GmbH, Jülich, Germany, p. 40.

[17] S. Lunardi, M. Ogawa, M.R. Maier, and P. Kleinheinz, Annual Report 1976, Institut für Kernphysik, Kernforschungsanlage Jülich GmbH, Jülich, Germany, p. 31.

[18] F. Schussler, R. Brissot, J. Crançon, E. Monnard, C. Ristori, and A. Moussa, Nucl. Phys. A209, 589(1973).

[19] J.T. Larsen, W.L. Talbert, Jr., and J.R. McConnell, Phys. Rev. C 3, 1372(1971).

[20] K. Heyde and P.J. Brussaard, Nucl. Phys. A104, 81(1967).

[21] G. Vanden Berghe, Z. Physik, A272, 245(1975).

[22] G. Vanden Berghe, private communication.

[23] P. Vogel and L. Kocbach, Nucl. Phys. A176, 33(1971).

[24] A. Arima and F. Iachello, Phys. Lett. 57B, 39(1975).

[25] T. Døssing, K. Neergård, K. Matsuyanagi and Hsi-Chen Chang, Phys. Rev. Lett. 39, 1395(1977).

[26] J. Kownacki, H. Ryde, V.O. Sergejev, and Z. Sujkowski, Nucl. Phys. A196, 498(1972).